Deep Discharge Characteristics of $LiMn_2O_{4-d}Cl_d$ Cathode Material

Terrill B. Atwater and Paula C. Latorre
US Army RDECOM
Communications, Electronics, Research, Development and Engineering Center
Aberdeen Proving Ground, MD 21005

Abstract: *A family of lithium manganese $AB_2O_{4-d}X_d$ materials was synthesized and evaluated as a cathode for lithium and lithium-ion electrochemical systems. The reversible region for the $Li//Li_xMn_2O_{4-d}Cl_d$ electrochemical couple was found to be on the order of $0.05 < x < 1.75$ in a two step thermodynamic charge-discharge profile. The high voltage twin plateau is centered on 3.95 volts and 4.35 volts and the low voltage plateau is centered on a potential of 2.85 volts. In comparison, $Li//Li_xMn_2O_4$ (non-doped lithium manganese-based AB_2O_4 spinel materials) needs to be maintained at $0.05 < x < 1.00$ and at a potential greater than 3.25 volts in order to maintain rechargeablity. Additionally, the ability to discharge the $Li//Li_xMn_2O_{4-d}Cl_d$ electrochemical system below 3.25 volts increases the capacity of the lithium spinel electrochemical couple nearly twofold.*

Keywords: $Li_xMn_2O_4$; Deep Discharge; Rechargeable Cells

Introduction

The benefits of lithium battery systems lie within their high energy density (Wh/L) and high specific energy (Wh/kg). Manganese dioxide (MnO_2) is an attractive active cathode material because of its high energy density and low material cost. MnO_2 is an intercalating compound for lithium that functions by solvating and desolvating lithium cations from the electrolyte in solid state. The lithium cations are deposited into the vacancies of the MnO_2 cathode crystal structure. The objective of this effort focuses on improving the cycle life of rechargeable lithium manganese-based electrochemical systems, specifically the capacity fading of the cathode. These two characteristics are still considered the major technology hurdles in rechargeable lithium battery technology.[1-4]

A family of lithium manganese $AB_2O_{4-d}X_d$ materials was synthesized and evaluated as a cathode for lithium and lithium-ion electrochemical systems. The general formula for the synthetic material is $Li_xMn_2O_{4-d}X_d$ where $x \approx 1$ and d ranges from 0.005 to 0.3. By introducing halogens into the starting material mixture and subsequently into the final product, the synthesis processing time of lithium manganese-based AB_2O_4 spinel materials is dramatically reduced. The material properties were verified with X-ray diffraction and X-ray fluorescence. Button cells were fabricated to evaluate thermodynamic and kinetic properties of the $Li//Li_xMn_2O_{4-d}X_d$ electrochemical systems. Results of these evaluations were reported previously and concentrated on the formulation processes and the 4.5 to 3.5 volt cycle window. [5-7]

During the development phase, $Li_xMn_2O_{4-d}X_d$ recovered electrochemically after deep discharge (a discharge to a 2.0 volt potential or lower). Deep discharges are routinely performed on developmental materials so that a complete electrochemical thermodynamic characterization can be established. It was discovered that deep discharges to 2.0 volts could be performed without any permanent damage to the electrochemical properties of the cell. It is this 3.5 to 2.0 volt region for the $Li//Li_xMn_2O_{4-d}X_d$ electrochemical systems that will be presented in this paper.

Background

Capacity fading is the loss of cycle capacity in a cell over the entire life of a battery system, limiting the practical number of cycles that may be used. In lithium battery systems, capacity loss is often attributed to the degradation of the active cathode material. This degradation is a result of both changes in composition and crystal structure of the active material that occurs during both charging and discharging of the cell. The crystal structure degradation is linked to the intercalation and deintercalation of lithium cations into the active material. Additionally, throughout the life of a cell, parasitic side reactions occur between the different chemical species of the cell. These include chemical dissolution and degradation of the active cathode material and oxidation-reduction of the electrolyte. Methods of reducing this effect include changing the crystal structure and composition of the active material or eliminating these parasitic mechanisms through other means. Capacity fading is currently a major setback for rechargeable lithium cells; therefore it is an active area of research.[2-12]

MnO_2 exists in different phase states or crystal structures. The common phases are referred to by the following prefixes: α, β, γ, and λ. α-MnO_2 is the most stable structure; it is a one-dimensional lattice containing both one-by-one and two-by-two channels for lithium insertion/extraction. γ-MnO_2 is a one-dimensional structure but has a one-by-two channel. λ-MnO_2 is created through the delithiation of Li-Mn-O type spinels ($Li_xMn_2O_4$). The crystal structure of the spinel is maintained through both delithiation and lithiation. The λ-MnO_2 crystal structure is a three-dimensional cubic array. This structure promotes mechanical stability and

adequate pathways for lithium insertion/extraction. λ-MnO_2 is perhaps the most preferred rechargeable phase of MnO_2. Degradation of the λ-MnO_2 crystal structure forming α/γ-MnO_2 and other Mn_xO_y phases reduces the capacity of the cathode material. [13-20]

As lithium intercalates, the size and orientation of the crystal structures change. In $Li_xMn_2O_4$ spinel materials, the crystal structure is cubic (λ-MnO_2) when $0.05 < x < 1$. When $1 < x < 1.8$, the structure of $Li_xMn_2O_4$ (no longer an AB_2O_4 spinel) is tetragonal. Additionally, when $x < 0.05$, a phase transition to the more stable α, β, and γ MnO_2 occur. Over-discharge of the $Li_xMn_2O_4$ spinel increased lithium insertion into the cathode, promoting the transformation of λ-MnO_2 crystal structures to other cubic, tetragonal, and monoclinic phases. The preferred transition is λ-MnO_2 to other cubic phases since tetragonal and monoclinic crystal structures may become inactive, leading to the loss of active cathode material. Voltage control allows for control of the formation of unwanted crystal structures. [13-17] When the potential of the Li//$Li_xMn_2O_4$ electrochemical system is maintained between 3.0 and 4.25 volts, the λ-MnO_2 cubic phase is maintained. As the potential of the system drops below 3.0 volts, the $Li_xMn_2O_4$ cathode material undergoes a phase change from cubic to tetragonal.[13-20]

This effort focuses on the formulation, fabrication, and characterization of manganese-based metal oxide materials as a positive electrode for lithium electrochemical systems, with the goal of improving the overall performance characteristics of the system. The limited cycle life and limited rate capability are considered the major setbacks in rechargeable lithium battery technology and are the focus of the efforts described in the manuscript. A stable chlorine-modified lithium manganese based AB_2O_4 spinel material was formulated, fabricated, and characterized as a positive electrode for lithium batteries. The general formula for the fabricated material is $Li_xMn_2O_{4-y}Cl_z$ where $x \approx 1$, $y \approx z$, and $0.005 < z < 0.3$. The reversible region for the Li//$Li_xMn_2O_{4-y}Cl_z$ electrochemical couple is $0.05 < x < 1.75$.

The chlorine-modified $Li_xMn_2O_4$ cathode material allows for over-discharge protection. Reversibility in the material is maintained after cell potential excursions less than 2.0 volts are performed. When the chlorine-modified $Li_xMn_2O_4$ cathode material is coupled with a lithium anode, it successfully cycles between 5.0 and 2.0 volts without significant degradation. Conventional $Li_xMn_2O_4$ cathode materials tend to degrade as a result of stress/strain-induced material fracture and formation of Mn_2O_3 and Mn_3O_4. This is due to the cubic to tetragonal and cubic to monoclinic phase changes as a result of the Mn^{3+} valence state. Both of these conditions occur as the electrochemical cell potential transitions through 3.0 volts.

Experimental

Hydrothermal and solid state processes were used to fabricate the $Li_xMn_2O_{4-d}X_d$ material, where $x \approx 1$ and d ranges from 0.005 to 0.3 with MnO_2 or Mn_2O_3 and Li_2CO_3 or LiOH as the principal starting materials. Halogens were introduced into the starting material mixture and subsequent final product using lithium and manganese halide salts. Mixtures were ground using a random orbit mixer mill and the subsequent material was then heated in air at 600°C for a time period no greater than 4 hours. The material was evaluated for its viability as a cathode material for rechargeable lithium batteries.

The material properties were verified with X-ray diffraction and X-ray fluorescence. Button and laboratory glass test cells with a lithium anode and an organic electrolyte were fabricated to evaluate the thermodynamic and kinetic properties of the Li//$Li_xMn_2O_{4-d}X_d$ electrochemical systems. The glass cell consisted of two machined pistons that are fitted into glass housings and secured with a threaded cap incorporating a pair of o-rings. The pistons, either aluminum, nickel, or stainless steel, had a surface area of 1.0 cm^2. The pistons served as electrode current collectors and are threaded, allowing for an inert captivating ring to be employed to maintain electrode alignment. The glass fixture allows for postmortem analysis of the cell components. Conventional button cells with a surface area of 2.85 cm^2 were also used.

The experimental cells were composed of a lithium anode separated from the cathode by a nonwoven glass separator. The $Li_xMn_2O_{4-d}X_d$ cathode was fabricated by mixing together the active material, carbon, and polytetrafluoroethylene with an 85:10:5 by weight ratio, respectively. The cathode mixture was rolled to 0.04 cm and dried in a vacuum oven. A 0.075 cm thick lithium foil was cut using a 12.7 mm or 19.0 mm diameter hole punch. The cathode was cut into 1.0 cm^2 and 2.85 cm^2 discs, resulting in a 0.05 g cathode for the glass cell and a 0.14 g cathode for the button cells. A 0.01 cm nonwoven glass separator was utilized for the separator and as a wick. The electrolyte used was 1 molar $LiPF_6$ in proportional mixtures of diethyl carbonate, dimethyl carbonate, and ethylene carbonate.

Cells were cycled with an ARBIN MSTAT4 battery cycler system controlled by MITS Pro software. The charge/discharge rates were maintained at 0.5 to 4.0 mA/cm^2, with the majority of electrochemical experiments cycled at 1.0 mA/cm^2. The cells were charged to a cut-off between 4.75 to 5.0 volts and discharged to a cut-off between 3.0 to 2.0 volts. A rest period of 15 minutes between charge and discharge cycles was used to allow for cells to achieve equilibrium on all experiments.

Results & Discussion

Figure 1 shows the molecular model of $Li_xMn_2O_{4-d}Cl_d$. The halogen element replaces an oxygen in the λ-MnO_2 structure. The impact of the halogen material on the entire structure is highly dependent on its concentration. For every chlorine atom inserted into the structure, it will influence the three adjacent manganese atoms and the twelve associated oxygen atoms. Once the concentration becomes too large where multiple chlorines are affecting the same central manganese atoms in a crystallite, the structure begins to reject the additional halogen. This was found to occur at $d = 0.3$

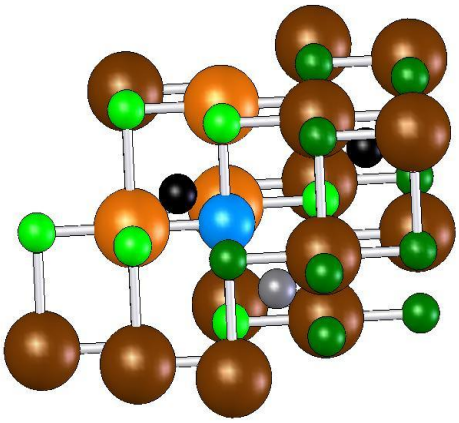

Figure 1. Molecular model of $Li_xMn_2O_{4-d}X_d$ with *x* being either Cl or F. The halogen element replaces an oxygen in the λ-MnO_2.

Figure 2 displays the results of a representative deep discharge experiment on a Li//$Li_xMn_2O_{4-y}Cl_z$ electrochemical cell where *z* is 0.05. For this experiment, a 125 uA/cm^2 charge/discharge cycle was interrupted every hour and the cell was allowed to rest for 15 minutes so that it could reach thermodynamic equilibrium. The data shows that the Li//$Li_xMn_2O_{4-y}Cl_z$ is fully reversible. This reversibility instigated further investigations into the behavior of the electrochemistry during cycles that routinely are cut off at 2.0 volts during discharge.

Figures 3 and 4 show the first three charge/discharge cycles of a representative Li//$Li_xMn_2O_{4-y}Cl_z$ electrochemical cell. Figure 3 displays the data as a potential verses time trace and Figure 4 displays the data as differential capacity. Figures 5 and 6 show data from the initial discharge/charge cycles of a representative Li//$Li_xMn_2O_{4-y}Cl_z$ electrochemical cell. Figure 5 displays the data as a potential verses time trace and Figure 6 displays the data as differential capacity. Comparison of data where charge verses discharge was used to initiate the formation cycle show significantly different behavior during the first cycle. Subsequent cycles, however, are comparable.

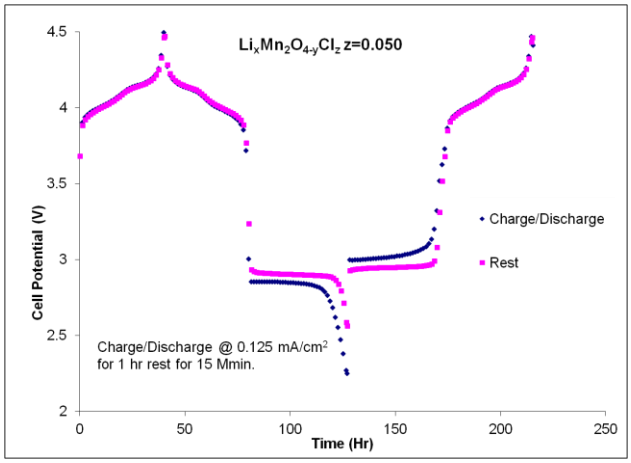

Figure 2. Cell potential data from an electrochemical thermodynamic experiment on a Li//$Li_xMn_2O_{4-y}Cl_z$ cell, where *z* is 0.05.

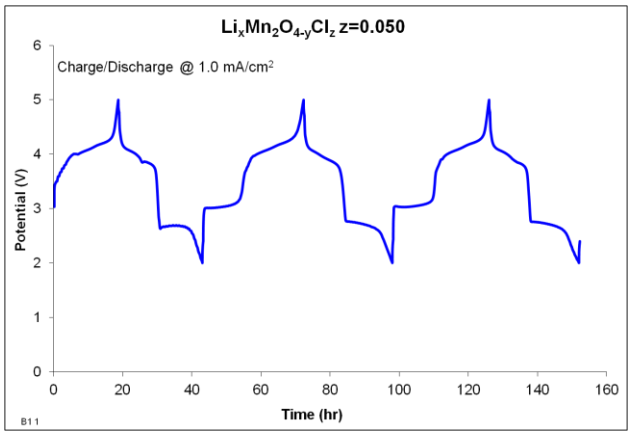

Figure 3. Cell potential data for a representative Li//$Li_xMn_2O_{4-y}Cl_z$ electrochemical cell during the forming, 2nd, and 3rd cycle.

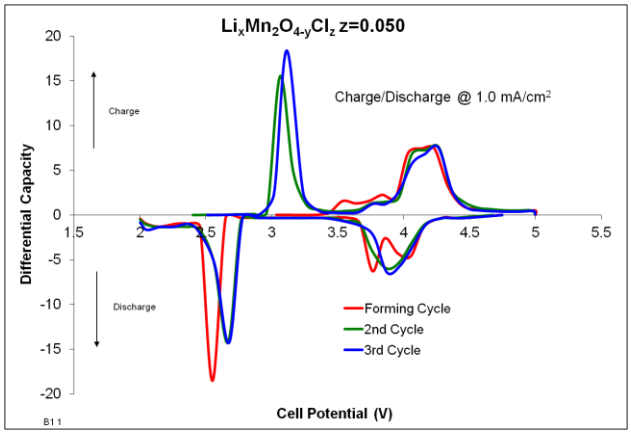

Figure 4. Differential capacity data for a representative Li//$Li_xMn_2O_{4-y}Cl_z$ electrochemical cell during the forming, 2nd, and 3rd cycle.

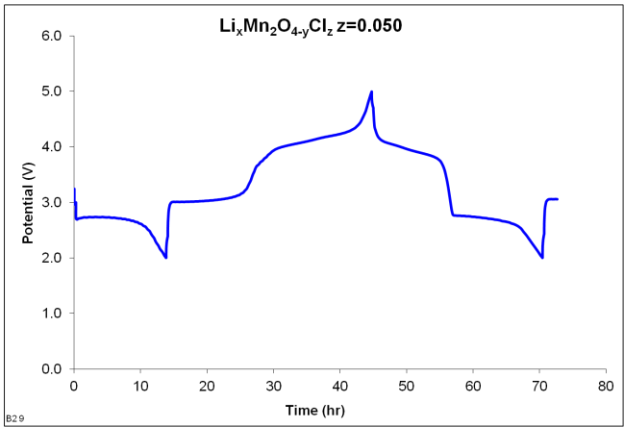

Figure 5. Cell potential data for a representative Li//$Li_xMn_2O_{4-y}Cl_z$ electrochemical cell where the initial cycles started with a discharge.

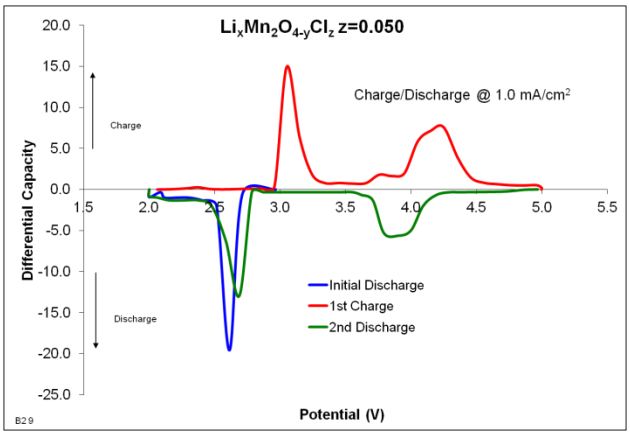

Figure 6. Differential capacity data for a representative Li//$Li_xMn_2O_{4-y}Cl_z$ electrochemical cell where the initial cycles started with a discharge.

Conclusion

A family of lithium manganese $AB_2O_{4-d}Cl_d$ materials was synthesized and evaluated as a cathode for lithium and lithium-ion electrochemical systems. The general formula for the material is $Li_xMn_2O_{4-d}Cl_d$ where $x \approx 1$ and d ranges from 0.005 to 0.3. By introducing halogens into the starting material mixture and subsequently into the final product, the synthesis process time of lithium manganese-based AB_2O_4 spinel materials is dramatically reduced. In addition to the reduction in formation time, the subsequent chlorine-modified material was evaluated for its viability as a cathode material for a rechargeable lithium battery. The reversible region for the Li//$Li_xMn_2O_{4-d}Cl_d$ electrochemical couple was found to be on the order of $0.25 < x < 1.75$ in a two-step thermodynamic charge-discharge profile. The high voltage twin plateau is centered on 3.95 volts and 4.35 volts and the low voltage plateau is centered on a potential of 2.85 volts.

The chlorine-modified $Li_xMn_2O_4$ cathode material allows for over-discharge protection. Reversibility in the material is maintained after cell potential excursions less than 2.0 volts are performed. When the chlorine-modified $Li_xMn_2O_4$ cathode material is coupled with a lithium anode, it successfully cycles between 5.0 and 2.0 volts without significant degradation. In comparison, Li//$Li_xMn_2O_4$ (non-doped lithium manganese-based AB_2O_4 spinel materials) needs to be maintained at $0.05 < x < 1.00$ and at a potential greater than 3.25 volts in order to maintain rechargeablity.

References

1. David Linden (Ed.); Handbook of Batteries 4th ed.; McGraw-Hill, 2011
2. Tarascon, JM, Guyomard D, *J. Electrochem Soc.*, Vol. 138, Oct. 1991, pg. 2864
3. Thackeray, MM, etal, *Mater Res. Bull.*, 1984, pg 179
4. Gabano, JP, Lithium Batteries; Academic Press; New York, NY; 1983
5. Atwater, TB and Tavares, P.C., *P. 45th Power Sources Conference*, 2012
6. Atwater, TB and Tavares, P.C., **US Patent No. 8,597,377**, December 3, 2013
7. Atwater, TB and Tavares, P.C., *SAE Int. J. Materials and Manufacturing*, 6(1):2013
8. Liu, W-R, et.al., *J. Power Sources*, 146 (2005) pg. 233-239
9. Kang, Y-J, et.al., *J. Power Sources*, 146 (2005) pg. 237-240
10. Kang, S-H, Goodenough JB, *J. Electrochem Soc.*, Vol. 147, No. 10, October 2000, pg. 3621-3627
11. Kang, S-H, Goodenough JB, *Electrochemical and Solid State Letters*, Vol. 3, No. 12, (2000), pg. 536-539
12. Sun, Y-K, et.al., *Electrochemical and Solid State Letters*, Vol. 3, No. 1, (2000), pg. 7-9
13. Inoue, T and Sano, M, *J. Electrochem Soc.*, Vol. 145, No. 11, November 1998, pg. 3704-3707
14. Larcher, D et.al.; *J. Electrochem Soc.*, Vol. 145, No. 10, October 1997, pg. 3392-3400
15. Wen, SJ et.al., *J. Electrochem Soc.*, Vol. 143, No. 6, June 1996, pg. L136-L138
16. Shao-Horn, Y et.al.; *J. Electrochem Soc.*, Vol. 144, No. 9, September 1997, pg. 3147-3153
17. Armstrong AR, et.al.; *J. Solid State Chem.*, Vol. 14, No.5 , 1999, pg. 549-556
18. Yang, XQ et.al., *Electrochemical and Solid State Letters*, Vol. 2, No. 4, (1999), pg. 157-160
19. Xia, Y and Yoshio, M, *J. Electrochem Soc.*, Vol. 143, No. 3, March 1996, pg. 825-833
20. Xia, Y et.al., *J. Electrochem Soc.*, Vol. 148, No. 7, July 2001, pg. A723-A729